ELSEVIER

Tectonophysics 289 (1998) 117–128

TECTONOPHYSICS

A note on induced stress changes in hydrocarbon and geothermal reservoirs

Paul Segall [a,*], Shaun D. Fitzgerald [b]

[a] *Department of Geophysics, Stanford University, Stanford, CA 94305, USA*
[b] *Department of Petroleum Engineering, Stanford University, Stanford, CA 94305, USA*

Received 2 April 1996; accepted 2 October 1996

Abstract

Earthquakes have been induced by oil and gas production, where pore pressures have *decreased*, in some cases by several tens of MPa. It has previously been suggested that such earthquakes are caused by poroelastic stressing of crust surrounding the reservoir. Induced earthquakes are also common in geothermal fields, such as The Geysers, where strong correlations between both steam production and condensate injection, and earthquake activity have been observed over the last several decades. Stress measurements within hydrocarbon reservoirs show that the least horizontal stress decreases with declining reservoir pressure, as predicted by poroelasticity. For circular disk-shaped reservoirs, isothermal reduction in pore pressure induces a relative horizontal tension within the reservoir. Production-induced stressing may promote frictional sliding on pre-existing faults. Within the reservoir itself, normal faulting is promoted if the regional stress is extensional and the Biot coefficient is sufficiently large, $\alpha > 0.85$ for reasonable coefficients of friction. On the other hand, dilatant fracturing and normal faulting are always promoted, in extensional environments, near the edge of the reservoir or in regions of high pore-pressure gradient. It is suggested that such fracturing could enhance fracture permeability in tight rocks adjacent to portions of the reservoir that experience large reductions in pore pressure due to production. In regional compressional environments, production modestly favors reverse faulting above and below the reservoir. The ratio of thermal to poroelastic stress can be quite large in geothermal reservoirs such as The Geysers. Reservoir-wide energy balance considerations suggest that the average temperature has declined at The Geysers by 6ºC during the past 20 years. Reservoir average stress changes are thus on the order of ~2 MPa, and are certainly much larger near injection wells and steam-producing fractures.

Keywords: stress change; hydrocarbon reservoir; geothermal reservoir

1. Introduction

There is now good empirical evidence that extraction of pore fluids from within the crust can trigger earthquakes (Yerkes and Castle, 1976; Pennington et al., 1986; Segall, 1989; Grasso and Wittlinger, 1990). Segall (1989) suggested that extraction-induced earthquakes are triggered by poroelastic stresses associated with reservoir contraction. Declining pore pressures cause reservoir rocks to contract slightly. Because the reservoir is elastically coupled to the surrounding rocks, this contraction stresses the neighboring crust. This results in subsidence, horizontal contraction above the reservoir, and in some instances, triggered seismicity.

Faulting associated with fluid withdrawal is illus-

* Corresponding author. E-mail: segall@pangea.stanford.edu

0040-1951/98/$19.00
PII S0040-1951(97)00311-9

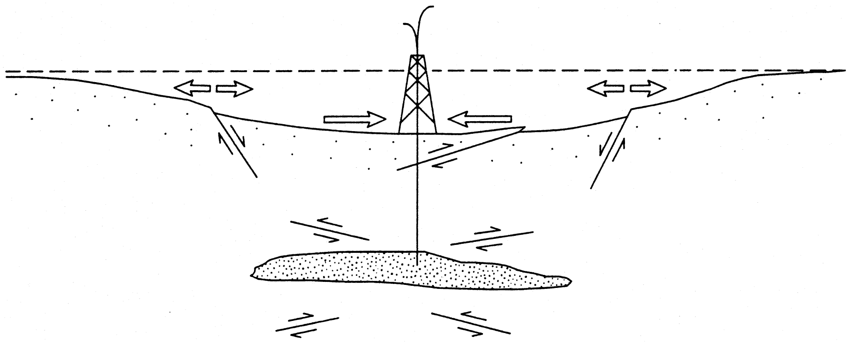

Fig. 1. Summary of observed faulting associated with fluid withdrawal. Open arrows indicate horizontal strain. Normal faults develop on the flanks of the field when the depleted reservoir is located in an extensional environment, whereas reverse faults develop above and below the reservoir in compressional environments. After Segall (1989).

trated schematically in Fig. 1. Note that induced faulting generally occurs outside the reservoir. It should also be emphasized that not all of the faults in Fig. 1 are developed in any given setting; the style of faulting depends on the ambient stress state. In extensional environments normal faults bounding the reservoir may be developed perpendicular to the least horizontal principal stress (e.g. the Goose Creek field, Texas; Pratt and Johnson, 1926). In compressional environments reverse faulting may be developed above or below the reservoir; e.g. the Buena Vista Hills field, California (Koch, 1933), and the Strachan field Alberta (Wetmiller, 1986), respectively.

Segall et al. (1994) compared subsidence and the spatial distribution of seismicity with predictions of poroelastic calculations for the Lacq gas field in southwestern France, assuming a radially symmetric reservoir. Perturbations in stress σ_{ij} due to changes in pore pressure p are computed by integrals of the form (Geertsma, 1973; Segall, 1992):

$$\sigma_{ij}(\mathbf{x}) = \alpha\frac{(1-2\nu)}{2(1-\nu)} \times \left[\int_V p(\mathbf{x}')G_{ij}(\mathbf{x},\mathbf{x}')\mathrm{d}V - p(\mathbf{x})\delta_{ij}\right] \quad (1)$$

where α is the Biot pore-pressure coefficient, ν is the drained Poisson ratio, G_{ij} are elastostatic Green's functions corresponding to centers of dilatation, and δ_{ij} is the Kronecker delta ($\delta_{ij} = 1$ for $i = j$, $\delta_{ij} = 0$ for $i \neq j$). Segall et al. (1994) computed subsidence based on a-priori knowledge of the reservoir geometry, pore-pressure decline, and material properties, and showed that the calculations were in good agreement with subsidence measured by repeated leveling surveys. They also compare the perturbing poroelastic stresses with the distribution of seismicity. The agreement was found to be reasonable, assuming that fault slip occurred on pre-existing surfaces that are optimally oriented for frictional sliding and that prior to production the least principal stress was vertical.

In this note we focus on stress changes occurring *within* hydrocarbon and geothermal reservoirs and their implications for reservoir properties and induced seismicity. Hydraulic fracturing measurements show that minimum horizontal stresses decrease (become more tensile) with decreasing reservoir pore pressure (Fig. 2). Teufel et al. (1991) demonstrated this for the Ekofisk field, where the ratio of change in horizontal stress to reservoir pore pressure is $\mathrm{d}\sigma_\mathrm{h}/\mathrm{d}p \sim 0.8$. Earlier, Salz (1977) (reported in Engelder and Fischer, 1994) had presented similar data for the McAllen Ranch, Texas field. A least-squares fit to all of the McAllen Ranch data (Fig. 2) yields $\mathrm{d}\sigma_\mathrm{h}/\mathrm{d}p \sim 0.5$.

While these observations have previously been recognized as a poroelastic effect, there has been some disagreement about how to interpret the data. Engelder and Fischer (1994) treat the reservoir as a horizontal layer and assume that production occurs with no net horizontal strain. This leads simply to:

$$\Delta\sigma_\mathrm{h} = \alpha\frac{1-2\nu}{1-\nu}\Delta p \quad (2)$$

(see below). Teufel et al. (1991), however, question whether constant-strain, or displacement, boundary conditions are appropriate and suggest that the actual boundary conditions may be intermediate between these two extremes.

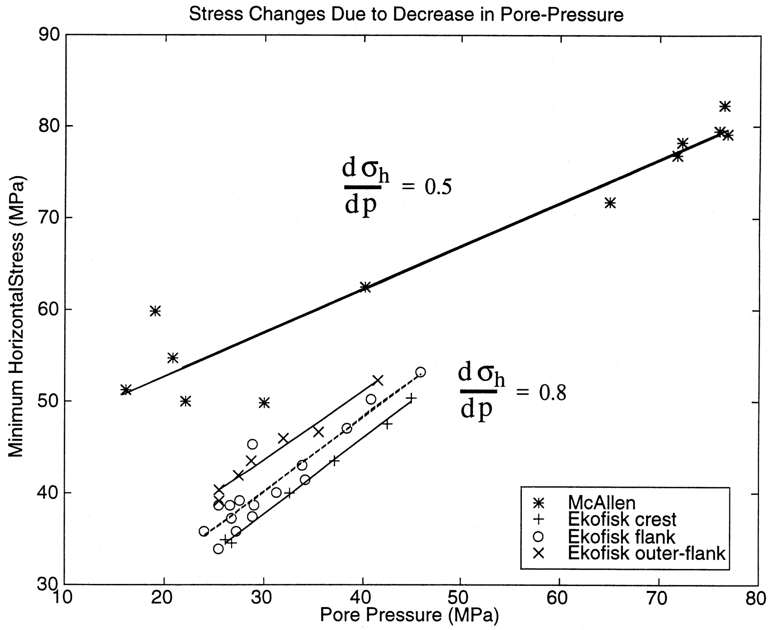

Fig. 2. Stress changes due to decrease in reservoir pore pressure. Horizontal axis is reservoir pore pressure. Vertical axis is minimum horizontal stress, as determined by hydraulic fracturing. Ekofisk data from Teufel et al. (1991). McAllen data from Salz (1977).

In this note we consider the reservoir to be an ellipsoidal inclusion embedded in an otherwise elastic continuum. It is thus the geometry of the reservoir and the elasticity of the surroundings that control the boundary conditions on the reservoir. Although idealized, such a model reasonably predicts the poroelastic fields inside the reservoir, as well as the surface strains and subsidence. In contrast, an infinitely extensive flat reservoir predicts spatially uniform subsidence and no horizontal strain above the reservoir. The latter is in contradiction to field observations. For example, at the Wilmington oil field in Long Beach, California, horizontal contractions reached 1% strain, causing pipelines and railroad tracks to buckle (Yerkes and Castle, 1976).

2. Method

Consider an ellipsoidal reservoir with semi-major axes $a_1 > a_2 > a_3$, embedded in a uniform full space (Fig. 3). For simplicity, free surface effects will be neglected in this analysis. We further assume that the pore pressure within the reservoir is reduced uniformly by Δp during production and that the temperature decreases uniformly by ΔT. The pore pressure and temperature outside the reservoir remain unchanged. The elastic properties of the reservoir and surrounding rocks are the same.

For a linear, isotropic, thermo-poroelastic medium the solid strain, ε_{ij}, depends on the stress, σ_{ij}, pore pressure, p, and temperature T, through (e.g. McTigue, 1986):

$$\varepsilon_{ij} = \frac{1}{2\mu}\sigma_{ij} - \frac{\nu}{2\mu(1+\nu)}\sigma_{kk}\delta_{ij} + \frac{1-2\nu}{2\mu(1+\nu)}\alpha(p-p_0)\delta_{ij} + \lambda(T-T_0)\delta_{ij} \quad (3)$$

where p_0 and T_0 are, resp., the pore pressure and

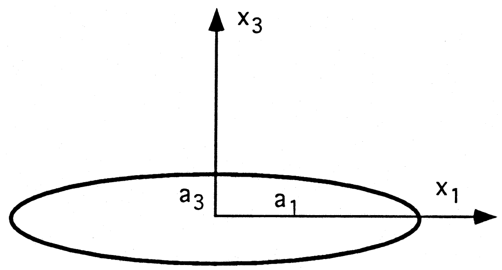

Fig. 3. Model reservoir with semi-major axes a_1, a_2, a_3 where $a_1 = a_2 > a_3$.

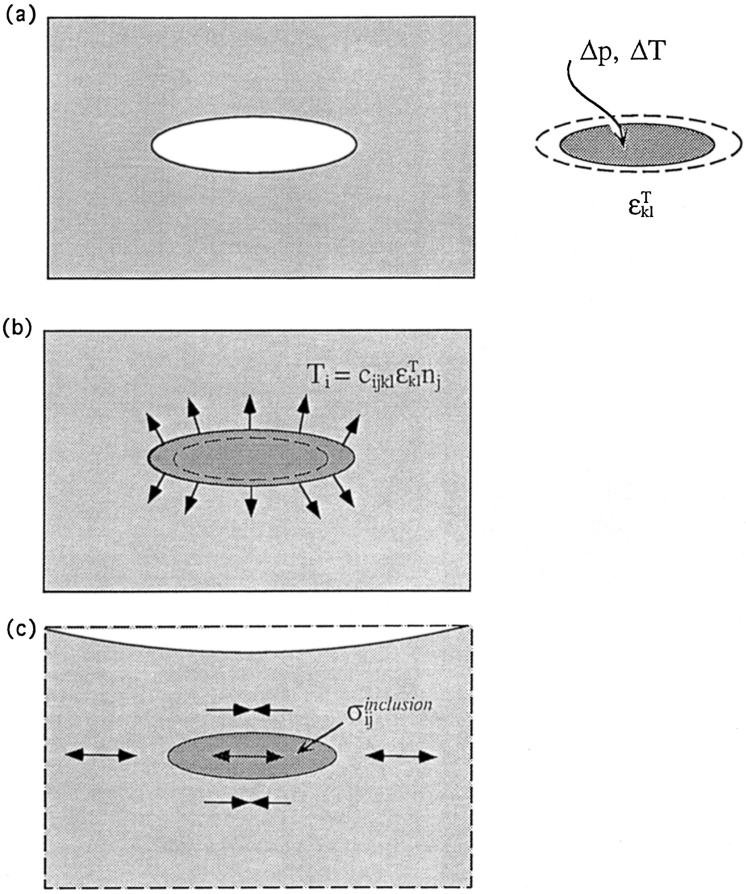

Fig. 4. Schematic illustrating the sequence of steps needed to compute the stress in the reservoir. (a) The ellipsoidal reservoir is removed from the earth. Fluid and heat are extracted causing the pore pressure and temperature to change by Δp and ΔT, respectively. This causes the reservoir to undergo a 'transformation' strain ε^{T}_{kl}. (b) Tractions are applied to the boundary of the reservoir such that the elastic strain is equal and opposite to the transformation strain. At this point the reservoir fits exactly back into the earth. (c) The reservoir is glued back in place and the surface tractions relaxed. This results in a uniform stress within the reservoir $\sigma_{ij}^{\text{inclusion}}$.

temperature in the reference (unstrained) state, μ and ν are, resp., shear modulus and Poisson's ratio under drained isothermal conditions, α is the Biot pore-pressure coefficient, and λ is the coefficient of linear thermal expansion. The Biot coefficient α relates the change in pore pressure to strain of the porous medium. If the porous matrix is compliant, in comparison to the solid constituents, then $\alpha \sim 1$, whereas if the matrix is very stiff $\alpha \sim 0$.

Assuming lateral constraint (zero horizontal strain), the stress change given by Eq. 2, is simply obtained from Eq. 3 for isothermal conditions, assuming the two horizontal normal stresses are equal and the vertical stress (change) is zero.

To compute the stresses within an ellipsoidal reservoir, we first imagine removing the reservoir from the elastic earth and uniformly reducing the pore pressure and temperature by Δp and ΔT within the reservoir (Fig. 4a). As there are no stresses applied to the boundary of the reservoir during this process, the change in pore pressure and temperature induces a 'stress-free' or 'transformation' strain, which from Eq. 3 is:

$$\varepsilon^{T}_{kl} = \frac{1-2\nu}{2\mu(1+\nu)}\alpha\Delta p\delta_{kl} + \lambda\Delta T\delta_{kl} \quad (4)$$

In order to restore the reservoir to its initial shape we apply tractions to the boundary (with magnitude

$-C_{ijkl}\varepsilon^T_{kl}n_j$, where n_j is the unit normal to the inclusion boundary, and the C_{ijkl} are the elastic constants) such that the elastic strain is equal and opposite to the transformation strain. This step is imagined to be done under drained, isothermal conditions so that the reservoir temperature and pore-pressure changes remain ΔT and Δp. The reservoir is now restored to its initial shape, although the elastic strain in the reservoir is $-\varepsilon^T_{kl}$, and fits exactly in its original position (Fig. 4b). We now 'glue' the reservoir back into the elastic earth and remove the applied boundary tractions (Fig. 4c). Eshelby (1957) showed that the resulting strain in the inclusion is given by:

$$\varepsilon^{\text{inclusion}}_{ij} = -\varepsilon^T_{ij} + S_{ijkl}\varepsilon^T_{kl} \tag{5}$$

where the S_{ijkl} are rank four tensors known as the 'Eshelby shape factors' (e.g. Mura, 1982). The second term on the right-hand side of Eq. 5 represents the constraint of the elastic surroundings applied to the reservoir.

From Eqs. 4 and 5 the *elastic* strain within the reservoir is given by:

$$\varepsilon^{\text{inclusion}}_{ij} = \left[\frac{1-2\nu}{2\mu(1+\nu)}\alpha\Delta p + \lambda\Delta T\right](S_{ijkk} - \delta_{ij}) \tag{6}$$

The inclusion stresses are then given by Eq. 3 for drained, isothermal conditions. This yields:

$$\sigma^{\text{inclusion}}_{ij} = -\left[\alpha\Delta p + 2\mu\frac{1+\nu}{1-2\nu}\lambda\Delta T\right]\Sigma_{ij} \tag{7}$$

where the Σ_{ij} are defined as:

$$\Sigma_{ij} \equiv \left(\delta_{ij} - \frac{1-2\nu}{1+\nu}S_{ijkk} - \frac{\nu}{1+\nu}S_{kknn}\delta_{ij}\right) \tag{8}$$

The Σ_{ij} embody the reservoir geometry since the shape factors are functions of the reservoir semi-major axes and Poisson's ratio:

$$S_{ijkl}(a_3/a_1, a_2/a_1, \nu)$$

3. Stress changes in hydrocarbon reservoirs

Consider the model reservoir to be an oblate ellipsoid with semi-major axes $a_1 = a_2 > a_3$, with the x_3 direction vertical (Fig. 3). The horizontal stress change ($\sigma_{11} = \sigma_{22}$) due to an isothermal reduction in pore pressure (from Eq. 7) is:

$$\sigma^{\text{inclusion}}_{11} = -\alpha\Delta p\Sigma_{11} \tag{9}$$

Note that the change in horizontal stress is proportional to the change in pore pressure: the proportionality dependent on the Biot coefficient and the reservoir geometry. The shape term Σ_{11} is shown in Fig. 5 for different aspect ratios. In the limit that the reservoir thickness is much less than the horizontal dimensions, $a_1 = a_2 \gg a_3$, it can be shown using results from Mura (1982) that:

$$\Sigma_{11} = \frac{1-2\nu}{1-\nu}\left(1 - \frac{\pi}{4}\frac{a_3}{a_1}\right) \tag{10}$$

and

$$\Sigma_{33} = \frac{\pi}{2}\frac{1-2\nu}{1-\nu}\frac{a_3}{a_1} \tag{11}$$

These approximations are quite good for $a_3/a_1 > 5$ (see Fig. 5). Note that in the limit that the reservoir is infinite in extent, $a_3/a_1 \to 0$, that Eqs. 9 and 10 reduce to the lateral constraint result of Engelder and Fischer (1994). This limit is not unreasonable; for example, at Ekofisk, we approximate $a_3/a_1 = 150$ m/4 km $= 0.04$ (Van den Bark and Thomas, 1980). For Poisson's ratio in the range of 0.15 to 0.20, Eqs. 9 and 10 together with the observed value of $\Delta\sigma_h/\Delta p \sim 0.8$ yield $\alpha \sim 1$, which is in good agreement with laboratory data reported by Teufel et al. (1991).

An interesting test of poroelastic stressing due to reservoir depletion, which to our knowledge has not been done, would be to measure the stress change immediately above the reservoir. As noted previously, while the horizontal stress within the reservoir decreases (becomes more tensile), the horizontal stress above and below the reservoir is predicted to become more compressive. This arises because the contraction of the reservoir pulls the adjacent rocks inward, driving them into compression. In our simple model the change in pore pressure is discontinuous at the reservoir boundary. This causes the stress tangential to the reservoir boundary to be discontinuous at the boundary (Goodier, 1937):

$$\sigma^{\text{inclusion}}_{\text{tt}} - \sigma^{\text{exterior}}_{\text{tt}} = -\frac{1-2\nu}{1-\nu}\alpha\Delta p \tag{12}$$

where σ_{tt} denotes the stress tangential to the reservoir boundary. Equilibrium requires the perpendicular component of the stress as well as the shear stress be continuous across the boundary.

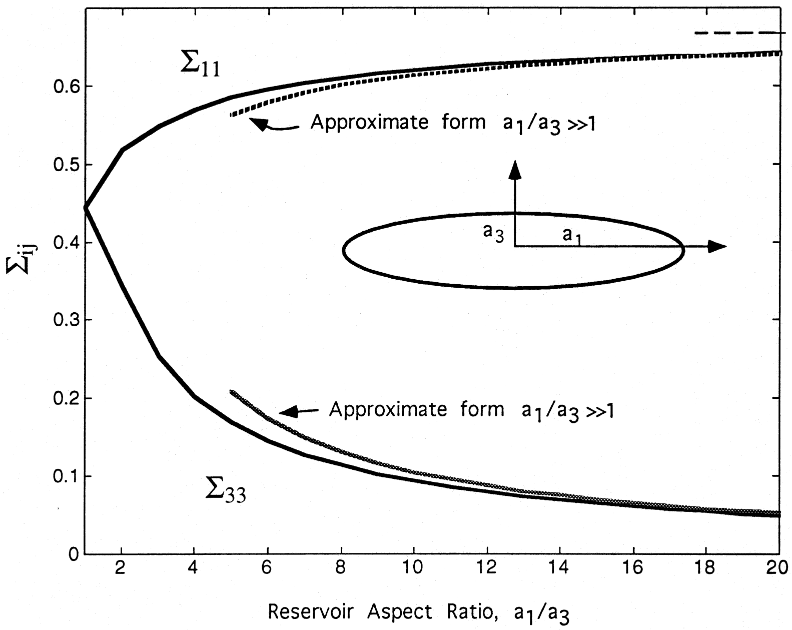

Fig. 5. Shape factors Σ_{11} and Σ_{33} as a function of reservoir aspect ratio $a_1/a_3 = a_2/a_3$. Poisson's ratio $\nu = 0.25$.

Immediately above the center of the reservoir the tangential stress is horizontal, and Eqs. 9 and 12 yield:

$$\Delta\sigma_{\mathrm{h}}^{\mathrm{exterior}} = \alpha\Delta p\left(\frac{1-2\nu}{1-\nu} - \Sigma_{11}\right) \qquad (13)$$

Note that as the reservoir pressure declines ($\Delta p < 0$) the horizontal stress above the reservoir becomes more compressive. In the limit $a_1 = a_2 \gg a_3$ Eq. 13 becomes:

$$\Delta\sigma_{\mathrm{h}}^{\mathrm{exterior}} = \alpha\Delta p\frac{1-2\nu}{1-\nu}\frac{\pi}{4}\frac{a_3}{a_1} \qquad (14)$$

The change in horizontal stress above and below the reservoir is thus opposite in sign and considerably smaller (by a factor of a_3/a_1) than the horizontal stress change within the reservoir. Because pore-pressure changes represent an internal source of stress, the integral of the horizontal stress change with depth must be zero. Thus, the relative tension within the narrow reservoir (half-depth a_3) is balanced by a smaller increase in compression spread over a much larger domain, with characteristic dimension a_1.

The situation is quite different at the edge (lateral boundary) of the reservoir. Because the normal component of the traction must be continuous at the boundary of the reservoir, the horizontal stress just outside the reservoir must be the same as that inside. The stress change outside the reservoir can thus be of order $\alpha\Delta p$, although it will decay rapidly with distance from the reservoir. Interestingly the *effective* stress change outside the reservoir is also of order $\alpha\Delta p$, as the pore-pressure change there is small. This may have important implications for induced faulting and fracturing as discussed in the following section.

4. Faulting and fracturing due to production

The effective stress for fracturing is:

$$\Delta\tilde{\sigma}_{ij} \equiv \Delta\sigma_{ij} + \Delta p$$

so that the change in the least compressive horizontal stress is:

$$\Delta\tilde{\sigma}_{\mathrm{h}} = \Delta p(1 - \alpha\Sigma_{11}) \qquad (15)$$

The quantity in parentheses is non-negative, so that $\Delta\tilde{\sigma}_{\mathrm{h}}$ is always negative when fluid is extracted from the reservoir. One thus expects vertical fractures oriented perpendicular to σ_{h} to contract during production.

In general the stresses outside the reservoir vary with position and can be computed from Eq. 1. It is possible to approximate the stress at the edge of the reservoir, however, by recalling that the horizontal stress must be continuous at the boundary. In the simple ellipsoidal model of the reservoir the pore pressure is discontinuous at the reservoir boundary. This suggests that dilatant (mode I) fracturing could be induced in the surroundings perpendicular to the least horizontal compression. In actuality the pore-pressure change must be continuous; however, the simple result should be applicable as long as the pore-pressure gradient is sufficiently steep. If the pore-pressure changes are abrupt the induced stresses can be significant. Reservoir pore-pressure changes can be on the order of 20 to 30 MPa or more (Fig. 2), and $\alpha\Sigma_{11}$ is of the order of one-half. From Eq. 9 the least compressive stress at the periphery of the reservoir may thus increase by 10 to 15 MPa.

Teufel et al. (1991) suggested that the production-induced stress changes can lead to normal faulting within the reservoir. Slip on a pre-existing fault becomes more likely as the Coulomb stress:

$$\Delta\Phi \equiv \Delta\tau + \mu_s \Delta\tilde{\sigma}_n \tag{16}$$

increases (recall tension is positive here). Here τ and $\tilde{\sigma}_n$ are the shear stress and effective normal stresses acting on the fault, and μ is the coefficient of friction. The horizontal effective stress change is given by Eq. 15. The vertical stress change is negligible, so that $\Delta\tilde{\sigma}_v \sim \Delta p$. If the reservoir is in a regional normal-faulting environment, that is the regional least compressive stress is horizontal, then Eq. 16 becomes:

$$\Delta\Phi = -\Delta p\{\alpha\Sigma_{11}\sin(\theta)[\cos(\theta) + \mu\sin(\theta)] - \mu\} \tag{17}$$

where θ is the fault dip. Declining pore pressure will favor normal faulting within the reservoir if:

$$\alpha > \frac{\mu}{\Sigma_{11}\sin(\theta)[\cos(\theta) + \mu\sin(\theta)]} \tag{18}$$

The critical value of α is shown in Fig. 6 as a function of μ and fault dip θ, for a Poisson ratio of $\nu = 0.20$, and a reservoir aspect ratio $a_1/a_3 \sim 26$ appropriate for the Ekofisk field. The in-situ stress data indicate that $\alpha \sim 1$ at Ekofisk, suggesting that normal faulting may be induced within the reser-

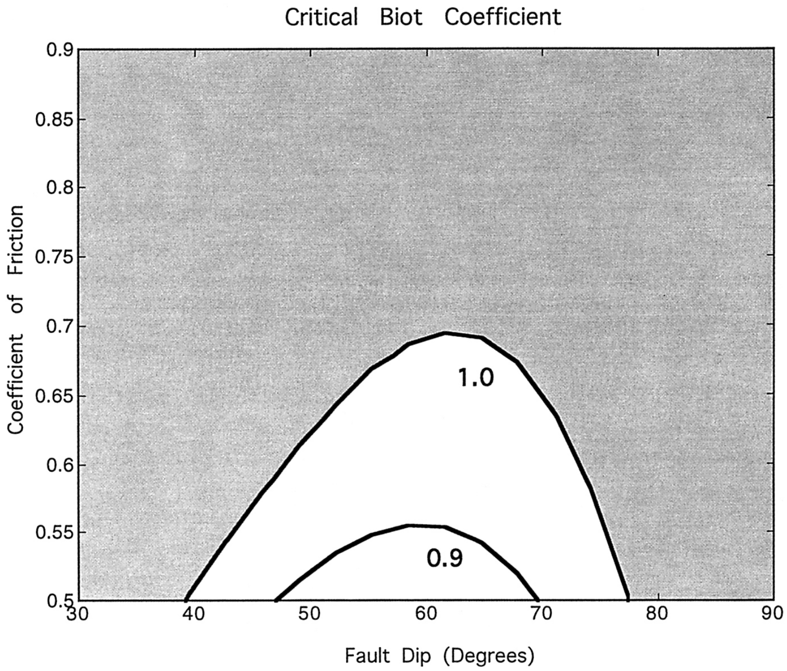

Fig. 6. Critical Biot coefficient for normal faulting to occur within the reservoir, for a range of fault dips (in degrees) and friction coefficients. Poisson's ratio $\nu = 0.2$; Reservoir aspect ratio $a_1/a_3 \sim 26$. The shaded area is not allowed, as the Biot coefficient is bounded by $0 \leq \alpha \leq 1.0$.

voir there. Note, however, that a rather large Biot coefficient is required for production to induce normal faulting within the reservoir. For the Poisson ratio and the reservoir aspect ratio used here, normal faulting is inhibited for $\alpha < 0.85$, assuming $\mu \geq 0.5$, or for $\mu > 0.7$ for arbitrary α.

Outside the reservoir, production does not directly decrease the pore pressure so that the tendency for normal faulting is considerably more pronounced. In this region the Coulomb stress change is:

$$\Delta\Phi = -\Delta p \alpha \Sigma_{11} \sin(\theta)[\cos(\theta) + \mu \sin(\theta)] \quad (19)$$

which is positive for all $\Delta p < 0$. This suggests that in extensional environments, normal faulting will be promoted near the edge of the reservoir or indeed anywhere there is a steep gradient in pore-pressure reduction. Eq. 19 neglects possible undrained pore-pressure changes outside the reservoir, which would occur in a half-space calculation. As discussed below, this effect is unlikely to alter the general behavior described here.

In a regional thrust faulting environment the reduction in horizontal compression stabilizes faults within the reservoir. Faults above or below the reservoir, however, will become less stable (Segall, 1989). It is possible to approximate the change in Φ immediately above or below the center of the reservoir, assuming again that the vertical stress does not change and the horizontal stress change is given by Eq. 13. We have assumed that the pore pressure does not change outside the reservoir. Compression of the rocks above and below the reservoir may lead to an increase in pore pressure there, if the permeability is sufficiently low that the deformation is essentially undrained. Increasing pore pressures in aquitards above pumped aquifers is known as the 'Noordbergum effect' in hydrology (Verruijt, 1969). This effect is not seen in full-space calculations, since the mean normal stress does not change outside the reservoir in a full space. In a more complete half-space calculation the drained pore-pressure response, appropriate for times short compared to characteristic pore-pressure diffusion times, is given by:

$$\Delta p = -B \frac{\sigma_{kk}}{3} \quad (20)$$

Here B is Skempton's pore-pressure coefficient, which depends on the compressibility of the rock, pores, and pore fluid, and is strictly bounded by $0 \leq B \leq 1$.

Assuming that the deformation is fully drained, and the horizontal stress change is given by Eq. 14 the change in Coulomb stress is:

$$\Delta\Phi = -\alpha \Delta p \frac{\pi}{4} \left(\frac{1-2\nu}{1-\nu}\right)\left(\frac{a_3}{a_1}\right) \times \sin(\theta)[\cos(\theta) - \mu \sin(\theta)] \quad (21)$$

For a fault dip of 30º, and similar parameters to those used above we find:

$$\Delta\Phi \sim -\frac{\alpha \Delta p}{6} \frac{a_3}{a_1}$$

For $\Delta p \sim -50$ MPa, $\alpha \sim 1$, and $a_3/a_1 \sim 0.04$, we find that $\Delta\Phi \sim 0.33$ MPa. Although modest, such perturbations can apparently trigger seismicity if the pre-existing regional stresses are sufficiently close to failure. Note, however, that neglecting the finite lateral extent of the reservoir, equivalent to the limit $a_3/a_1 \rightarrow 0$ predicts no change in horizontal stress outside the reservoir and thus no tendency for faulting.

The tendency for faulting to occur within and adjacent to reservoirs is summarized in Fig. 7. In extensional environments, normal faulting is promoted within the reservoir if the Biot coefficient is sufficiently large. Normal faulting is favored near the periphery of the reservoir in extensional environments for all values of α and μ. In compressional environments, reverse faulting is promoted above and below the reservoir, with magnitude that scales with $-\alpha \Delta p \ (a_3/a_1)$.

The tendency for extensional fracturing and normal faulting associated with abrupt changes in pore pressure may have implications for changing reservoir properties during production. One can speculate that steep gradients in pore pressure due to lateral variations in permeability might generate substantial changes in horizontal stress that favor extensional fracturing and normal faulting in the lower-permeability medium. This might lead naturally to enhanced fracture permeability in just those regions that have naturally low permeability. Perhaps this can account for the observation at Ekofisk that reservoir permeability has not declined with production, despite significant reservoir compaction and subsidence (Teufel et al., 1991).

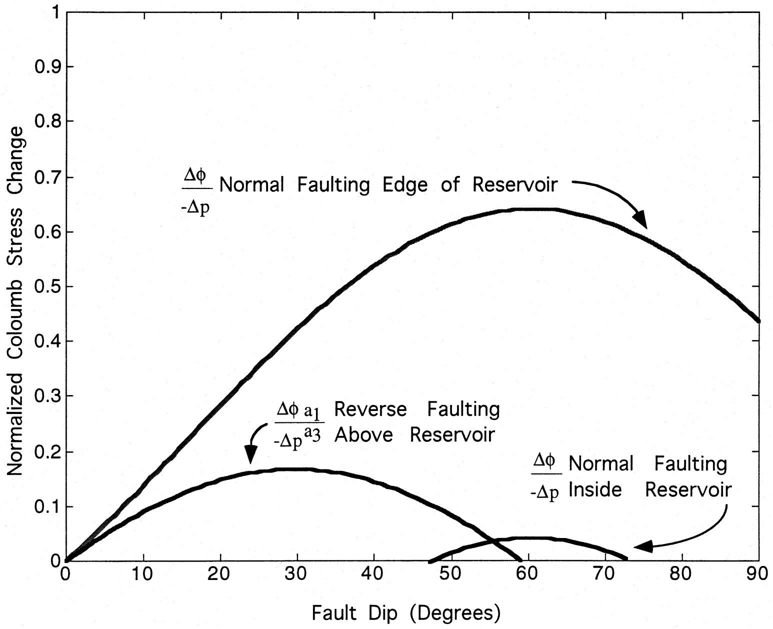

Fig. 7. Change in Coulomb condition $\Delta\Phi$ normalized by reservoir pressure drop $-\Delta p$ for various faulting geometries. For the case of reverse faulting above the reservoir the Coulomb change is normalized by reservoir aspect ratio a_3/a_1. Calculations are for Poisson's ratio $\nu = 0.2$, Biot coefficient of 1.0, and reservoir aspect ratio $a_1/a_3 \sim 26$.

5. Stress changes in geothermal reservoirs

Production from geothermal reservoirs at saturated conditions results in a decline in both reservoir pressure and temperature. As an example of the effects of decreasing temperature and pore pressure on the state of stress within geothermal reservoirs, we will consider The Geysers steam field in north-central California. The Geysers is one of the largest producing geothermal fields in the world, with installed generating capacity that peaked at 2000 MW (Gambill, 1992). Steam is produced at temperatures of 225° to 255°C from Franciscan graywackes and an underlying silicic intrusive. Within the reservoir, water is stored in the liquid phase within matrix porosity, which averages only 2%. During production, hot water flashes to steam in response to the decreased pressure and flows through a network of fractures to the producing wells. As production continues the zone of pressure drop expands and the boiling zone spreads away from the well. Steam flow is dominated by fracture permeability, which is estimated to be 10–180 mD, far greater than the matrix permeability of 5–120 μD (Barker et al., 1992).

Beginning in 1987 steam production at The Geysers began to decline. The decline is attributed to a drop in reservoir pressure rather than from loss of heat. Since the beginning of exploitation, steam pressure has dropped by 2.2 MPa (from an estimated initial value of 3.5 MPa to as little as 1.3 MPa in 1988; Barker et al., 1992). To combat the decline in pore pressure approximately one third of the steam condensate is reinjected into the reservoir.

The Geysers is also one of the most seismically active areas in northern California (Hill et al., 1990). Most workers agree that much of the seismicity is induced. However, there is little unanimity about the dominant mechanism. Oppenheimer (1986) noted strong spatial and temporal correlation between seismicity at The Geysers and steam production. Majer and McEvilly (1979) suggested that volumetric strains associated with steam production might cause the microseismicity. Denlinger and Bufe (1982) suggested that shear stresses induced by depressuring steam-filled fractures trigger the seismicity. Alternatively, Allis (1982) suggested that production causes a transition between (previously undetected) aseismic deformation and stick-slip deformation.

More recently, Stark (1992) found a good correlation between the location of injection wells and epicenters of events with depths greater than 4000 ft. (~1219 m). Shallower events apparently do not correlate with injection. Stark (1992) also reports a temporal correlation between the onset of injection in a particular area and an increase in seismicity rate. He notes, however, that only roughly half of the earthquakes at The Geysers are simply related to injection.

We can use the results of Eq. 7 to quantify the relative size of thermoelastic and poroelastic stresses due to production in geothermal reservoirs:

$$\frac{\sigma_{ij}^{\text{thermo}}}{\sigma_{ij}^{\text{poro}}} = \frac{K\lambda}{\alpha}\frac{\Delta T}{\Delta p} \tag{22}$$

where K is bulk modulus. The linear coefficient of thermal expansion is typically in the range $\lambda \sim 0.5 - 1.0 \times 10^{-5}$°C^{-1} (Skinner, 1966). Seismic velocities in The Geysers (Majer and McEvilly, 1979) imply bulk moduli of $K \sim 3 \times 10^4$ MPa. As previously noted α is bounded between 0 and 1, and is typically in the range $\alpha \sim 0.5 - 1.0$. Thus, the coefficient term in Eq. 22 is bounded by 0.1 MPa/°C $< K\lambda/\alpha <$ 2 MPa/°C, and is likely to be on the order of 0.4 MPa/°C at The Geysers (assuming $\alpha \sim 0.75$).

As liquid water and steam coexist within fractures, the most obvious way to estimate $\mathrm{d}T/\mathrm{d}P$ then is from the slope of the vapor pressure (coexistence) curve, which is $\mathrm{d}T/\mathrm{d}P \sim$ 19°C/MPa at ~3 MPa. According to this argument, Eq. 22 implies that thermal stresses exceed poroelastic stresses by a factor of 8 or more (the slope of the vapor-pressure curve increases with decreasing pressure).

It is important to note, however, that these pressure and temperature changes are restricted to the neighborhood of steam-producing fractures. Due to capillary effects, the pressure change within matrix pores may be far less than that within steam-filled fractures. The reservoir averaged pore-pressure change is therefore likely to be small and poroelastic effects negligible.

The large temperature changes implied by the slope of the Clausius–Clapeyron curve are also restricted to the neighborhood of producing fractures, and are not representative of the reservoir as a whole. A better estimate of the reservoir averaged temperature change is obtained from a net energy balance for the reservoir. Energy conservation applied to the reservoir requires:

$$V\rho c\frac{\mathrm{d}T}{\mathrm{d}t} = -Q \tag{23}$$

where V is the reservoir volume, ρ and c are the density and specific heat of the rock, T is temperature, and Q is the net flux out of heat out of the reservoir. Note that due to the low porosity, essentially all of the thermal energy is contained within the solid phase. In this analysis we consider only production-induced flux of heat into and out of the reservoir. This is equivalent to assuming either that prior to geothermal production the system was at steady state, or that the natural fluxes of heat in or out of the reservoir are small compared to those induced by geothermal production.

The net flux of steam out of the reservoir has averaged 3×10^{10} kg/year over the last 20 years (Barker et al., 1992). With an enthalphy of 2.8×10^6 J/kg (Pruess et al., 1987) this represents an energy loss of 8.4×10^{16} J/year. Approximately 35% of the steam is returned to the reservoir as liquid water at roughly 40°C. The specific heat of water is 4.2×10^3 J kg^{-1} °C^{-1}, so that 0.2×10^{16} J/year are returned to the reservoir via injection. The net energy loss of the reservoir is thus 8.2×10^{16} J/year. The volume of the reservoir that has undergone significant production is roughly 100 km^3. Taking $\rho = 2.6 \times 10^3$ kg/m^3, and $c = 920$ J kg^{-1} °C^{-1} (Pruess et al., 1987), yields $\dot{T} = -0.3$°C/year, or a net temperature decline of 6°C over 20 years.

While 0.3°C/year is a modest temperature change, and may very well be below the resolution of temperature measurements in The Geysers, it is sufficient to generate significant thermoelastic stresses. Using $K \sim 3 \times 10^4$ MPa, and $\lambda \sim 1.0 \times 10^{-5}$°C^{-1}, the estimated cooling rate corresponds to a stressing rate of 0.09 MPa/year (nearly 1 bar/year), or ~2 MPa when averaged over 20 years. Stress changes of this magnitude can induce earthquakes in critically stressed crust.

As emphasized above, the temperature and stress alterations are to be interpreted as reservoir averages. The temperature change within the reservoir is extremely non-uniform, with large concentrations near injection wells and steam-producing fractures. A more detailed analysis is required to model thermal stresses on these scales. Mossop and Segall (1997) show that thermoelastic stresses generated from injection of cold fluids into hot rock are quite appreciable. The calculations presented here simply illustrate that thermoelastic stressing cannot be ignored in geothermal reservoirs and is quite likely the dominant effect in altering the stress state within the reservoir. This suggests that microseismicity within The Geysers reflects temperature changes and may be useful in monitoring cold injectate within the reservoir.

6. Conclusions

Stress changes within reservoirs can be predicted if the appropriate poroelastic constants are known. Production may induce normal faulting within reservoirs if the Biot pore-pressure coefficient is sufficiently large. Dilatant fracturing and normal faulting can be induced by steep gradients in pore pressure and may act to enhance fracture permeability in tight rocks that serve as barriers to flow. In regional compressional environments, production may trigger reverse faulting above and below the reservoir. Thermoelastic effects dominate poroelastic stressing in geothermal reservoirs. Reservoir-wide stress changes in The Geysers steam field due to production-induced cooling average ∼2 MPa over the life of the field. Thermal stresses are likely to be much larger near injection wells and steam-producing fractures.

Acknowledgements

We thank Tony Mossop for valuable discussions and comments on the manuscript. This research was supported by the D.O.E. Office of Basic Energy Sciences.

References

Allis, R.G., 1982. Mechanism of induced seismicity at the Geysers geothermal reservoir, California. Geophys. Res. Lett. 9, 629–632.

Barker, B.J., Gulati, M.S., Bryan, M.A., Reidel, K.L., 1992. Geysers reservoir performance. In: Monograph on the Geysers geothermal field. Geothermal Resources Council, Spec. Rep. 17, pp. 167–178.

Denlinger, R.P., Bufe, C.G., 1982. Reservoir conditions related to induced seismicity at The Geysers steam reservoir, northern California. Bull. Seismol. Soc. Am. 72, 1317–1327.

Engelder, T., Fischer, M.P., 1994. Influence of poroelastic behavior on the magnitude of minimum horizontal stress, Sh, in overpressured parts of sedimentary basins. Geology 22, 949–952.

Eshelby, J.D., 1957. The determination of the elastic field of an ellipsoidal inclusion, and related problems. Proc. R. Soc. A241, 376–396.

Gambill, D.T., 1992. Recovery of injected water as steam at The Geysers. In: Monograph on the Geysers geothermal field. Geothermal Resources Council, Spec. Rep. 17, pp. 159–163.

Geertsma, J., 1973. Land subsidence above compacting oil and gas reservoirs. J. Pet. Technol. 25, 734–744.

Goodier, J.N., 1937. On the integration of the thermoelastic equations. Philos. Mag. 7, 1017–1032.

Grasso, J.R., Wittlinger, G., 1990. 10 years of seismic monitoring over a gas field area. Bull. Seismol. Soc. Am. 80, 450–473.

Hill, D., Eaton, J.P., Jones, L.M., 1990. Seismicity, 1980–86. In: The San Andreas Fault System, California. U.S. Geol. Surv. Prof. Pap. 1515.

Koch, T.W., 1933. Analysis and effects of current movements on an active fault in the Buena Vista Hill oil field, Kern County, California. Am. Assoc. Pet. Geol. Bull. 17, 694–712.

Majer, E.L., McEvilly, T.V., 1979. Seismological investigations at the geysers geothermal field. Geophysics 44, 246–269.

McTigue, D.F., 1986. Thermoelastic response of fluid-saturated porous rock. J. Geophys. Res. 91, 9533–9542.

Mossop, A., Segall, P., Subsidence at The Geysers geothermal field, N., 1997. California from a comparison of GPS and leveling surveys. Geophys. Res. Lett. 24, 1839–1842.

Mura, T., 1982. Micromechanics of Defects in Solids. Martinus Nijhoff, The Hague, 494 pp.

Oppenheimer, D.H., 1986. Extensional tectonics at The Geysers geothermal area, California. J. Geophys. Res. 91, 11463–11476.

Pennington, W.D., Davis, S.D., Carlson, S.M., DuPree, J.D., Ewing, T.E., 1986. The evolution of seismic barriers and asperities caused by the depressuring of fault planes in oil and gas fields of south Texas. Bull. Seismol. Soc. Am. 76, 939–948.

Pratt, W.E., Johnson, D.W., 1926. Local subsidence of the Goose Creek oil field. J. Geol. 34, 577–590.

Pruess, K., Celati, R., Calore, C., Cappetti, G., 1987. On fluid and heat transfer in deep zones of vapor-dominated geothermal reservoirs. In: Proc., 12th Workshop Geothermal Reservoir Engineering, January 20–22, Stanford Univ., Stanford, CA, pp. 89–96.

Salz, L.B., 1977. Relationship between fracture propagation pressure and pore pressure. Soc. Pet. Eng. Pap. SPE 6870, pp. 1–9.

Segall, P., 1989. Earthquakes triggered by fluid extraction. Geology 17, 942–946.

Segall, P., 1992. Induced stresses due to fluid extraction from axisymmetric reservoirs. Pure Appl. Geophys. 139, 535–560.

Segall, P., Grasso, J.R., Mossop, A., 1994. Poroelastic stressing

and induced seismicity near the Lacq gas field, southwestern France. J. Geophys. Res. 99, 15423–15438.
Skinner, B.J., 1966. Thermal Expansion. In: Handbook of Physical Constants. Geol. Soc. Am. Mem. 97, 75–96.
Stark, M.A., 1992. Micro earthquakes — a tool to track injected water in The Geysers geothermal reservoir. In: Monograph on The Geysers geothermal field. Geothermal Resources Council, Spec. Rep. 17, pp. 111–117.
Teufel, L.W., Rhett, D.W., Farrell, H.E., 1991. Effect of reservoir depletion and pore pressure drawdown on in situ stress and deformation in the Ekofisk field, North Sea. In: Rogiers, J.-C. (Ed.), Rock Mechanics as a Multidisciplinary Science. Balkema, Rotterdam, pp. 63–72.
Van den Bark, E., Thomas, O.D., Ekofisk, 1980. First of the giant oil fields in western Europe. In: Hablbouty, M.T. (Ed.), Giant Oil and Gas Fields of the Decade 1968–1978. Am. Assoc. Pet. Geol. Mem. 30, 195–224.
Verruijt, A., 1969. Elastic storage of aquifers. In: De Wiest, R.J.M. (Ed.), Flow Through Porous Media. Academic Press, New York, pp. 331–376.
Wetmiller, R.J., 1986. Earthquakes near Rocky Mountain House, Alberta and their relationship to gas production. Can. J. Earth Sci. 23, 172–181.
Yerkes, R.F., Castle, R.O., 1976. Seismicity and faulting attributable to fluid extraction. Eng. Geol. 10, 151–167.